Immobilization of Nucleic Acids at Solid Surfaces: Effect of Oligonucleotide Length on Layer Assembly

A. B. Steel,* R. L. Levicky,† T. M. Herne,‡ and M. J. Tarlov‡

*Gene Logic Inc., Gaithersburg, MD 20878; †Department of Chemical Engineering and Applied Chemistry, Columbia University, New York, NY 10027; and ‡Process Sensing Group, National Institute of Standards and Technology, Gaithersburg, MD 20899 USA

ABSTRACT This report investigates the effect of DNA length and the presence of an anchoring group on the assembly of presynthesized oligonucleotides at a gold surface. The work seeks to advance fundamental insight into issues that impact the structure and behavior of surface-immobilized DNA layers, as in, for instance, DNA microarray and biosensor devices. The present study contrasts immobilization of single-stranded DNA (ssDNA) containing a terminal, 5′ hexanethiol anchoring group with that of unfunctionalized oligonucleotides for lengths from 8 to 48 bases. Qualitatively, the results indicate that the thiol anchoring group strongly enhances oligonucleotide immobilization, but that the enhancement is reduced for longer strand lengths. Interestingly, examination of the probe coverage as a function of strand length suggests that adsorbed thiol-ssDNA oligonucleotides shorter than 24 bases tend to organize in end-tethered, highly extended configurations for which the long-term surface coverage is largely independent of oligonucleotide length. For strands longer than 24 bases, the surface coverage begins to decrease notably with probe length. The decrease is consistent with a less ordered arrangement of the DNA chains, presumably reflecting increasingly polymeric behavior.

INTRODUCTION

Micro-analytical methods for the investigation of biomolecules (e.g., nucleic acids, proteins) are rapidly evolving from proof-of-concept experiments into robust measurement systems for high-throughput analysis. A great deal of effort has been made to develop multiplex DNA sensors, so-called DNA chips (Cheung et al., 1999; Duggan et al., 1999; Lipshutz et al., 1999). At the core of DNA chip technology are arrays of single-stranded DNA (ssDNA) chains, or probes, that are tethered to a substrate for capture of complementary analyte DNAs, or targets. For DNA chip technology to continue to emerge as an alternative to conventional DNA diagnostic methods, questions about the conformation and activity of DNA at surfaces must be addressed (Kelley et al., 1997; Chan et al., 1997; Williams et al., 1994).

The two predominant methods of producing surface-immobilized probes are direct, on-chip synthesis of nucleic acids (Pease et al., 1994; Southern et al., 1994) and attachment of presynthesized oligonucleotides that are chemically modified to effect surface immobilization (O'Donnell et al., 1997; Gingeras et al., 1987). Although the former method presents an elegant approach to chip fabrication, it requires resources and expertise that can limit facile implementation. Therefore, use of presynthesized probes modified with an appropriate linking group is common. Irrespective of how DNA chips are fabricated, a greater understanding of the factors influencing the structure of immobilized DNA layers is needed to design surfaces exhibiting greater biological activity and selectivity.

One suitable model system for fundamental studies consists of thiol-containing probes that are immobilized through self-assembly to gold surfaces, as recently employed by several investigators (Bamdad, 1997; Levicky et al., 1998; Herne and Tarlov, 1997; Peterlinz et al., 1997). For example, scanning tunneling microscopy images of DNA oligonucleotides on gold have reported that single-stranded DNA (ssDNA) appeared as "blobs," whereas double-stranded DNA (dsDNA) was rodlike (Rekesh et al., 1996). Typically, ssDNA probes are attached to the gold surface through a sulfur-gold linkage. Recent neutron reflectivity studies indicated that on bare gold, ssDNA oligonucleotides form a compact layer— a picture that is consistent with the presence of multiple contacts between each strand and the substrate (Levicky et al., 1998). DNA nucleotides can presumably adsorb to gold via multiple amine moieties, as amines are known to chemisorb weakly to gold surfaces (Xu et al., 1993; Leff et al. 1996). Such adsorption at multiple sites can interfere with hybridization of the immobilized strands. As a remedy, the accessibility of immobilized probes to complementary target sequences can be enhanced by treating the surface with a small-molecule blocking agent, 6-mercapto-1-hexanol (MCH). The thiol group of MCH rapidly displaces the weaker adsorptive contacts between DNA nucleotides and the substrate, leaving the probes tethered primarily through the thiol end groups. After MCH treatment, the initially compact ssDNA swells and extends further into solution (Levicky et al., 1998). The less constrained tethering geometry renders the probes highly accessible to target, with nearly complete hybridization efficiencies observed (Steel et al., 1998).

As an extension of previous work, we have continued to explore key factors that influence oligonucleotide assembly

Received for publication 21 December 1999 and in final form 24 April 2000.

Address reprint requests to Adam B. Steel, Ph.D., Gene Logic, Inc., 708 Quince Orchard Road, Gaithersburg, MD 20878. Tel.: 301-987-1826; Fax: 301-987-1701; E-mail: asteel@genelogic.com.

0006-3495/00/08/975/07 $2.00

and organization on gold. This article addresses thiol-modified and native nucleic acid assembly as a function of ssDNA length in the range of 8 to 48 nucleotides.

EXPERIMENTAL

Materials

DNA oligonucleotides were purchased from Research Genetics (Huntsville, AL).[1] Probes of lengths 8, 12, 16, 24, 32, and 48 bases were synthesized with a 6-mercaptohexyl linker on the 5′ end for specific attachment to gold. The nucleic acid sequence was a repeated non-self-complementary 4-base unit, ACTG. Probes of the same lengths given above were also synthesized without the 6-mercaptohexyl linker. Oligonucleotides were labeled with α-^{32}P ddATP (Amersham International, Piscataway, NJ) in the presence of terminal deoxynucleotidyl transferase (Life Technologies, Gaithersburg, MD). The product was purified using a Sep-Pak C18 solid phase extraction column (Waters, Medford, MA), dried under vacuum centrifugation, and resuspended in 1 M phosphate buffer. 6-Mercapto-1-hexanol (MCH) was purified using flash chromatography (silica, chloroform) to remove traces of the corresponding dithiols. Hexaammineruthenium (III) chloride (99%; Strem Chemical, Newburyport, MA) was used as received. All other reagents were acquired from Sigma-Aldrich (St. Louis, MO). Solutions were made with deionized water (18 MΩ·cm resistivity) from a Barnstead NANOpure system.

Instrumentation

All electrochemical characterizations were performed in a single-compartment cell with a 10-mL volume. The working electrodes were prepared as described below. A saturated calomel electrode (SCE) and platinum wire gauze served as the reference and counter electrodes, respectively. Supporting electrolyte, 10 mM Tris, pH 7.4 (E-BFR), was deoxygenated via nitrogen purge for 10 min before measurements, and the cell was blanketed with nitrogen throughout the experiment. Cyclic voltammetry (CV) and chronocoulometry (CC) were performed with a CH Instruments (Cordova, TN) Model 660 electrochemical analyzer.[1] The following parameters were employed: CV, sweep rate = 100 mV/s; CC, pulse period = 500 ms, pulse width = 500 mV. Ultraviolet-visible spectra were obtained on a Cary Bio 300 spectrophotometer (Varian, Walnut Creek, CA). A Cyclone storage phosphor system with Super Sensitive storage screens (Packard Instrument Co., Meriden, CT) was used to obtain quantitative radioisotope measurements. All experiments were carried out at laboratory ambient temperature (21–24°C).

Substrate Preparation

Gold substrates were prepared by rf sputter deposition of *ca.* 200 Å of a chromium adhesion layer followed by *ca.* 2000 Å of gold (each 99.99% purity) onto glass microscope slides. Substrates were cleaned by exposure to warm piranha (70% sulfuric acid/30% peroxide) solution for 10 min, then rinsed thoroughly with deionized water. (WARNING: piranha reacts violently with organics.) Cleaned substrates were placed in monolayer deposition solutions while still wet.

DNA-modified surfaces were prepared using previously described procedure (Herne and Tarlov, 1997). Briefly, mixed monolayer surfaces containing thiolated probe ssDNA and MCH were prepared by first immersing the clean gold substrate in 400 μL of a 1.0-μM solution of probe oligonucleotide in 1.0 M potassium phosphate buffer (pH 7.0) for a specific time period, rinsing with 10 mM NaCl, 5 mM TRIS, pH 7.4, (R-BFR) for 5 s, immersing in 400 μL of 1.0 mM MCH solution in deionized water for 1 h, rinsing with R-BFR for 5 s, and drying under a stream of nitrogen. In all cases, the amount of probe in the deposition solution was at least 100 times greater than necessary to cover the active area of the substrate. As described in the Results and Discussion section, variants of this procedure were performed to study the effect of certain steps on probe immobilization.

Quantitation of DNA

Probe immobilization levels were quantitatively determined by either an electrochemical or radioisotopic method. In the electrochemical method, the probe coverage was calculated from the number of cationic redox molecules electrostatically associated with the anionic DNA backbone. A detailed description of the method has been presented elsewhere (Steel et al., 1998). Briefly, when an electrode modified with probe DNA is placed in a low ionic strength electrolyte containing a multivalent redox cation, the redox cation exchanges with the native DNA counterions and accumulates at the electrode. The amount of the accumulated redox cation can then be measured using chronocoulometry, a current integration technique, under equilibrium conditions (Bard and Faulkner, 1980). Specifically, the surface accumulation of redox cations attributed to the presence of immobilized DNA is determined from the difference in chronocoulometric intercepts for identical potential step experiments in the presence and absence of redox cation, e.g., ruthenium (III) hexaamine. The DNA surface density is calculated as the product of the redox cation surface density and the stoichiometric ratio of the redox cation charge to the number of phosphate residues in a nucleic acid probe. Electrochemical determination of probe surface coverage was used only after a sample was treated with MCH. Formation of the MCH monolayer served to reduce the double layer charging, thus improving the accuracy with which the probe coverage could be measured.

Quantitative radioisotopic measurements were performed by constructing calibration curves for each labeling reaction. Aliquots of radiolabeled probe deposition solution were prepared on filter paper at levels that spanned the anticipated surface density range from 1×10^{10} to 1×10^{14} molecules. The calibration curve and samples were exposed to the phosphor storage screen together. Values obtained with the radioisotopic and electrochemical methods were mutually consistent. For instance, the electrochemically determined probe surface density for a 16mer sample was $1.46 (\pm 0.13) \times 10^{13}$ strands/cm^2 (average and standard deviation of three samples); for the same sample, the isotopically determined probe surface density was 1.59×10^{13} strands/cm^2 (average of two samples).

RESULTS AND DISCUSSION

The evolution of surface coverage with adsorption time (5 min to 20 h) was investigated for thiolated probe with 8 to 48 nucleotides. These experiments were performed using the electrochemical method, in which probe density was determined after MCH treatment. Adsorption curves were used to estimate the maximal probe surface densities that can be attained after MCH treatment for each probe length and to determine the times needed to produce surfaces with desired probe densities. Reproducibly producing tailored surfaces is of particular importance for DNA chips, as the probe density plays a crucial role in the extent of subsequent target hybridization (Bamdad, 1997; Southern et al., 1999; Steel et al., 1998; Herne and Tarlov, 1997). Fig. 1 shows data for adsorption of the 16mer probe from a 1 μM solution. The coverage steeply increases during the first hour. After 2 h the coverage is 80 percent of that attained at 20 h. These results suggest that further increases in probe coverage are minimal with exposure times >20 h, and,

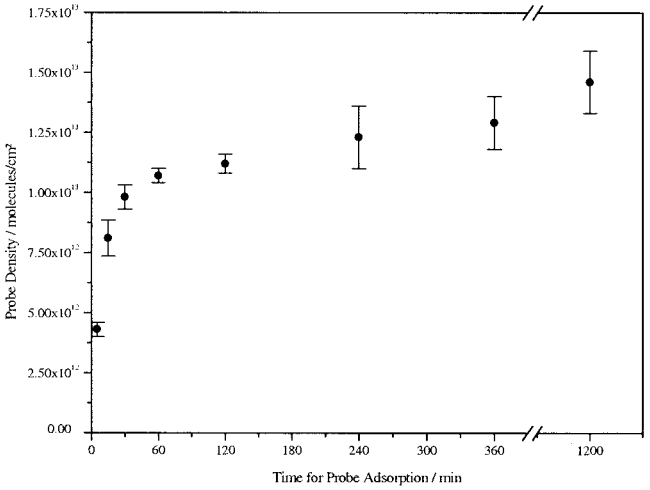

FIGURE 1 Surface density of 5′ thiol-modified 16mer oligonucleotide on gold after 6-mercapto-1-hexanol (MCH) treatment as a function of deposition period. Probe densities were determined electrochemically. The probe, sequence 5′-thiol-ACT-GAC-TGA-CTG-ACT-G-3′, was deposited from a 1 μM solution for the indicated time, followed by exposure to 1 mM MCH for 1 h. The error bars represent the standard deviation on at least three independent determinations per deposition time.

therefore, DNA adsorption periods of 20 h were used in the data presented below.

Experiments were also performed to examine the effect of DNA solution concentration on probe surface coverage. As shown in Fig. 2 for isotopically labeled 8mer probes, a 100-fold increase in probe concentration does not significantly alter the final coverage attained. When the concentration of a 48mer was increased from 1 to 10 μM, only a slight increase, 25%, in the surface coverage is observed (data not shown). The insensitivity of the final coverage to increased probe concentration supports the notion that the surface is unable to adsorb significantly more DNA. Although the adsorbed amount appears to saturate on the order of 1 day, it is possible that equilibration of long DNA probes is a not achieved in 20 h, the adsorption period used here. For example, adsorbed layers of long polymers can take months or more to equilibrate (Cohen Stuart and Fleer, 1996); such long-term processes were not investigated in these experiments.

A more complete understanding of the probe assembly process was gained by determining the surface coverage values before and after the MCH treatment for a range of probe lengths. As the electrochemical method requires the presence of MCH layer for reliable quantitation, probe surface densities were measured using phosphorimaging of radiolabeled samples. The adsorption of thiolated and native probes was compared to ascertain the contribution of the thiol in immobilization. Surface coverage values for thiolated and native probes, before and after MCH treatment, are plotted in Fig. 3. We first consider the data before the MCH treatment.

Dependence of Surface Coverage on Probe Length before MCH Treatment

Thiolated probes (filled circles in Fig. 3) with lengths between 8 and 48 nucleotides achieve surface coverage values that are at least an order of magnitude greater than those of the non-thiolated probes (filled squares). The driving force

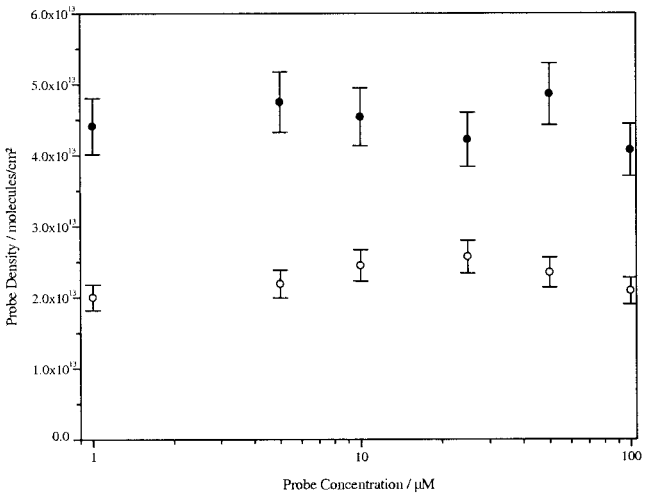

FIGURE 2 Probe density of 5′ thiol-modified 8mer oligonucleotide on gold as a function of the deposition concentration. Probe densities were measured before *(filled circles)* and after *(open circles)* MCH treatment (1 mM, 1 h) using phosphorimaging. The probe, 5′-thiol-ACT-GAC-TG-3′, was deposited from the indicated concentration for 20 h. The error bars represent the standard deviation on at least three independent determinations.

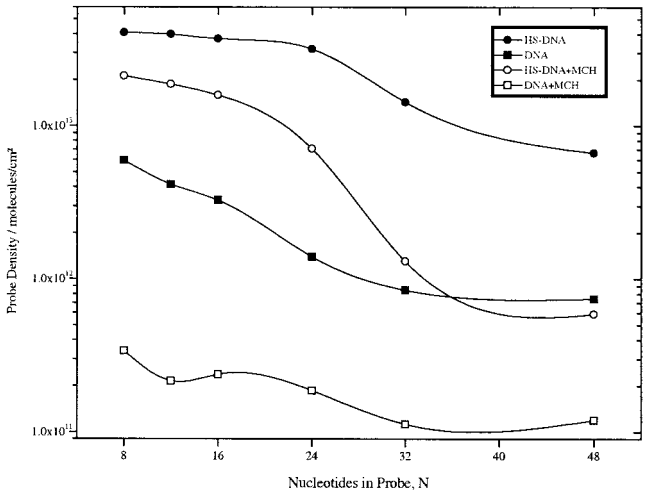

FIGURE 3 Probe density of radiolabeled oligonucleotides on gold as a function of modification and the number of nucleotides in the probe determined using phosphorimaging. Probe densities were measured before *(filled symbols)* and after *(open symbols)* MCH treatment (1 mM, 1 h). Data is shown for thiolated *(circles)* and non-thiolated *(squares)* oligonucleotides. Each value is an average of at least two independent determinations. Lines are meant only as a visual guide.

for the higher coverages of thiolated probes is presumably due to the formation of strong thiol-gold bonds (chemisorption energy of ≈30 kcal/mol; Ulman, 1996). A comparison of theoretical and experimentally determined coverages also indicates that thiol-gold bond formation is a strong driving force for immobilization and ordering of shorter probes. The cross-sectional radius of a ssDNA chain is estimated as 0.6 to 0.7 nm (Mucic et al., 1996; Rekesh et al., 1996). Close-packed ssDNA strands with this radius oriented normal to the surface would be present at a surface density of 6×10^{13} to 9×10^{13} probes/cm^2. This calculated value likely overestimates the maximum coverage, because it does not take into account additional steric requirements of counterions and water of hydration (Record et al., 1978). Experimentally, the surface densities for probes shorter than 24 nucleotides range from 3×10^{13} to 4×10^{13} probes/cm^2 (Fig. 3). The reasonable agreement between calculated and experimental coverages indicates that the energetically favorable thiol-gold interaction leads to dense packing of shorter probes in an extended configuration. Fig. 4 also shows that as probe length increases past 24, the difference between surface coverages for thiolated and unmodified probes begins to decrease. This is expected: as length increases, the effect of a single thiol group on probe immobilization becomes less significant when compared to the large number of adsorptive nucleotide-gold interactions that arise between each probe and the substrate. In addition, the entropic penalty associated with probe ordering will increase with increasing probe length. In the limit of infinitely long ssDNA strands, no difference in the adsorption of thiol-terminated and native chains would be expected. In practice, the length at which the thiol ceases to play a significant role will be finite and perhaps could be estimated by extrapolation from data on shorter probes; however, the range of lengths explored in the current study is too limited to allow such an extrapolation.

The variation of surface coverage with probe length provides insight into probe organization. Two models, displayed schematically in Fig. 4, representing the simplest scenarios, are considered: (I) probes are aligned normal to the surface in rodlike configurations, and (II) the probes pack as non-interpenetrating flexible coils. Model I should be applicable for short probes. In this model, the area occupied by a probe at the surface is given by the cross-sectional area of the ssDNA backbone and is independent of the number of nucleotides. Therefore, the surface density of probes should be independent of probe length. Model II would be applicable for longer probes that behave as flexible, coil-like polymer chains that adsorb side by side on the surface with no lateral interpenetration between coils. The effective footprint for each probe can be calculated from the radius of gyration R_g for a coil-like ssDNA strand. Under high salt conditions, the radius of gyration is estimated by $R_g = 0.38N^{1/2}$ nm, where N is the number of nucleotides in the strand (Tinland et al., 1997). The probe surface density is then proportional to the reciprocal of the effective cross-section of a probe coil, $1/R_g^2$, corresponding to an inverse dependence on N, i.e., probe surface density $\propto 1/N$.

In comparing the models to the data in Fig. 3, we consider only data acquired before the MCH treatment. From the surface density data for thiolated probes (filled circles in Fig. 3), a region of relative independence on N exists for $N < 24$ nucleotides. As discussed above, this observation is consistent with the notion of a close-packed layer of ssDNA rods, as represented by model I. Model I no longer applies once the entropic cost associated with constraining probes to the rod-like configurations dominates the adsorption energy; in this limit, the probes are so long that coiling commences and surface coverages decrease due to the larger footprints of the coiled DNA molecules. For probe lengths greater than 24 nucleotides, the thiolated probe surface density (filled circles in Fig. 3) exhibits a weak $1/N$ dependence as predicted for flexible coil behavior described by model II. Flexible coil behavior (i.e., $R_g \sim N^{1/2}$) has been measured for ssDNA, 280 to 5380 nucleotides long, in high ionic strength solutions where the Debye length is on the order of a few Angstroms (Tinland et al., 1997). Although the ionic strength in the current experiments is comparable, the probes are significantly shorter and likely do not attain the asymptotic behavior observed for longer chains. Indeed, difficulties with using model II to interpret the N-dependence of surface coverage are readily apparent. For example, the probe coverage should extrapolate to zero in the limit of infinite N. Fitting the present surface coverage data to $1/N$ dependence requires that the data be offset by a constant; therefore, the fit does not extrapolate to zero as N approaches infinity. Also, the underlying assumption of model II that adsorbed ssDNA probes do not interpentrate laterally can be neither proved nor disproved based on the present level of analysis. It is probable that probes from 24 to 48 nucleotides are in a transition regime, so that asymp-

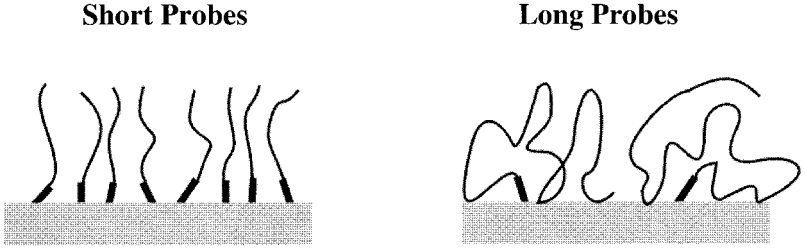

FIGURE 4 Cartoon of two packing configurations for ssDNA probes at a surface with a sticky endgroup for specific immobilization. Short probes are envisioned to pack in extended configurations. Longer probes are expected to exist in more flexible, polymeric-like configurations.

totic behavior of longer strands does not yet apply. Further studies are needed to characterize the relationship between surface coverage and probe length for long probes.

For the non-thiolated probes (filled squares in Fig. 3), there is no region in which the probe surface density is independent of probe length. As non-thiolated probes do not possess a sticky thiol endgroup, they are not driven to adsorb in the end-attached configurations presumed in model I. Instead, the probes are expected to adsorb in more flattened configurations with multiple contacts to the substrate. The surface coverage decreases with N over the entire range investigated, dropping by about an order of magnitude from $\sim 6 \times 10^{12}$ probes/cm^2 for 8mer probes to $\sim 7 \times 10^{11}$ probes/cm^2 for 48mers. A decreasing trend with probe length is expected, as it takes fewer large probes to cover a unit area of the substrate.

Taken together, the results provide compelling evidence that the presence of the thiol terminus is influential in the assembly and organization of ssDNA probes at gold surfaces. In summary, the surface coverage of thiolated probes is (1) about 1 order of magnitude greater than for native probes over the entire regime of probe lengths investigated, (2) independent of probe length for probes shorter than 24 bases with observed surface densities of around 4×10^{13} probes/cm^2, relatively close to the theoretical maximum of $\sim 8 \times 10^{13}$ probes/cm^2, and (3) strongly dependent on N for probes longer than 24 bases. These conclusions apply before the MCH treatment. Next, the changes in surface coverage arising from the MCH treatment will be considered.

Dependence of Surface Coverage on Probe Length after MCH Treatment

When adsorbed probe layers are exposed to MCH in deionized water, a significant fraction of both thiolated and non-thiolated ssDNA was displaced from the gold substrate (open symbols in Fig. 3). Both thiolated and non-thiolated ssDNA coverages are expected to decrease when exposed to MCH solutions because (1) adsorptive contacts between nucleotides on the ssDNA and gold are displaced by the formation of the stronger bond between the thiol group of MCH and the gold (Herne and Tarlov, 1997; Levicky et al., 1998), (2) electrostatic repulsions between adsorbed ssDNA strands are stronger in the deionized MCH solution than in the phosphate buffer used for the initial adsorption, driving some of the strands to desorb, and (3) for thiolated probes, the sulfur-gold bond between ssDNA and the substrate can be exchanged for one between MCH and the substrate, i.e., thiol-thiol exchange (Cotton et al., 1998; Tarlov et al., 1993). Most likely, all three of these contributions play a role. For thiolated probes, the MCH treatment is expected to leave some probes attached through their 5′ hexanethiol linker. For native ssDNA, nearly all strands are expected to be displaced by MCH.

As seen in Fig. 3, the surface density for the thiol-modified oligonucleotides (open circles) remains higher than that for the native ssDNA (open squares) for all probe lengths. For probes shorter than 16 bases, surface coverages of thiolated oligonucleotides are nearly two orders of magnitude greater than those of the unmodified ssDNA. However, for probes longer than 16 nucleotides this difference rapidly diminishes, dropping to only about a fivefold enhancement for thiolated 48mers. The fractional surface coverage, defined as the ratio of coverages after and before MCH treatment, for thiolated probes shows a marked decrease with increasing probe length. In contrast, the fractional surface coverage for native probes increases with probe length from about 5% for 8mers to 16% for 48mers, indicating that longer strands are more difficult to desorb from the gold surface. This result is expected because longer probes have more segments that can potentially interact with the surface, and disruption of all molecule-surface contacts is required for removal of DNA strands from the surface.

Due to the presence of the thiol group, the behavior of thiolated probes is expected to be more complicated. To determine which factors govern desorption of thiolated probes during MCH treatment, several control experiments were performed. Because, as previously discussed, the organization of thiolated layers is described by two length regimes, probes shorter and longer than 24 bases, the experiments included a probe from each length regime.

First, the need for MCH to be present to effect probe displacement was investigated for thiolated 12mers and 48mers. DNA was adsorbed for 20 h and then placed in deionized water with or without 1 mM MCH for 1 h. The fraction of remaining probes, relative to initial (pre-MCH) surface coverage, is displayed in Fig. 5. In deionized water (dH_2O), the fraction of probes remaining was 0.72 for the 12mer and 0.73 for the 48mer. When 1mM MCH was also present (MCH, dH_2O), the remaining fraction decreased to 0.47 for the 12mer and to 0.16 for the 48mer. These results indicate that MCH plays a significant role in displacing adsorbed probes from bare gold. In other words, displacement cannot be attributed solely to desorption of probes brought

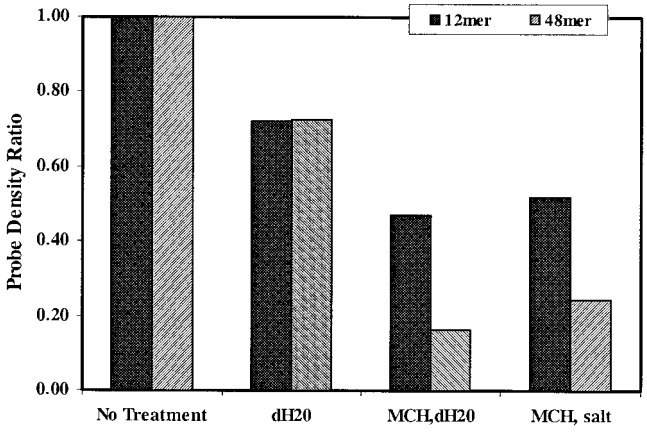

FIGURE 5 Probe density ratio before and after the indicated treatment (see text) for 5′ thiol modified 12mer and 48mer oligonucleotides. Each value is an average of at least two independent determinations.

about by, for example, electrostatic repulsions between adsorbed probes in deionized water.

Second, to further study the effect of electrostatic repulsion on final probe coverage, the ionic strength of the MCH treatment step was varied. Thiolated 12mer and 48mer samples were placed for 1 h in 1mM MCH solution to which sodium chloride was added at 1 M concentration. The results are also in Fig. 5. For both probe lengths, nearly as much probe desorbed in the 1M NaCl solution (MCH, salt) as when MCH in deionized water was used (MCH, dH_2O). Therefore, in comparison to the displacement effected by the formation of the MCH monolayer, electrostatic repulsion is not a dominant factor in determining final surface coverage for the probe lengths investigated.

Third, the effect of MCH exposure time on thiolated DNA displacement was investigated for thiolated 8mer and 48mer samples. The length of exposure to MCH is expected to impact the probe density if thiol-thiol exchange is a kinetically slow process. Initial displacement of thiolated DNA 8mer is rapid with the post-MCH to pre-MCH surface coverage fraction decreasing to 0.67 ± 0.05 ($n = 3$) at 10 min and 0.64 ± 0.04 ($n = 3$) at 1 h for the 8mer. After 20 h of exposure to MCH, only a small decrease is observed in the surface coverage fraction, 0.57 ± 0.05 ($n = 3$), for 8mer. In contrast, the displacement of longer strands by MCH is a much slower process. The 48mer surface density decreases roughly fourfold by increasing the treatment time from 1 to 20 h from 0.12 ± 0.02 ($n = 3$) to 0.03 ± 0.01 ($n = 3$) surface coverage fraction. The difference in reduction of surface coverage for the two probe lengths upon increasing MCH exposure from 1 to 20 h highlights that desorption can be a slow process for longer probes, and that equilibrium is not attained.

From the above experiments, the following interpretation can be formulated. As discussed earlier, before the MCH step the short probes (probe length <24 bases) are packed at surface coverages that are on the order of the maximum attainable; therefore, relatively few nucleotide-gold interactions are operative, and the probes must be attached predominantly through the thiol endgroups. Probe desorption during the MCH treatment step must then be a result of thiol-thiol exchange, rather than thiol displacement of nucleotide-gold contacts. Furthermore, at the high initial surface densities the desorption is also aided by electrostatic repulsions between adsorbed probes (cf. Fig. 5, data in dH_2O). Because electrostatic repulsion between probes lessens as probe surface density diminishes, the rate of desorption may be expected to decrease with time, as observed (third control experiment above). In addition, thiol-thiol exchange is also expected to slow due to steric constraints that arise as the MCH monolayer forms. Initially, surface sites around each probe are vacant and many directions are available from which incoming MCH molecules can attack and displace a thiol-gold bond between a probe and the substrate. As the MCH monolayer fills in, each probe becomes hemmed in by MCH molecules bound to neighboring sites on the substrate; therefore, attack of the probe-substrate bond by incoming MCH molecules becomes sterically hindered, slowing down probe desorption.

For thiolated probes longer than 24 nucleotides, the organization of the initially adsorbed probe layer is less understood. Experiment shows that the pre-MCH surface coverage values (filled circles in Fig. 3) begin to decrease notably with probe length. In contrast to the organization of shorter probe layers, for probes longer than about 24 nucleotides, multiple points of interaction are anticipated between a probe and the substrate that include thiol-gold as well as nucleotide-gold contacts. Upon treatment with MCH solution, the nucleotide-gold interactions are displaced, and a significant fraction of the initially adsorbed probes desorb. A few explanations for the greater propensity to desorb with increasing probe length can be postulated. First, the loss of stabilization energy from the nucleotide-gold interactions may lead to greater desorption because the thiol-gold interaction alone is insufficient to maintain the surface density. Second, the thiol-gold bond of longer probes may be more susceptible to thiol-thiol exchange by MCH because of the less dense molecular packing relative to the shorter probes. Finally, as the length of the thiolated probe increases, the probability of sulfur-gold bond formation decreases due to improper or constrained orientation of adsorbed DNA molecules. In the final scenario, the surface before MCH treatment contains a mixture of DNA molecules with and without a thiol-gold bond. Molecules with a thiol-gold bond will be more difficult to displace, whereas molecules without it will be easier to displace. For sufficiently long probes, we speculate that the thiol group will no longer be a significant factor and the surface density of thiolated and unmodified probes should converge to the same value. The data in Fig. 3 already indicate the beginning of this convergence (open circles and open squares). Immobilization of longer nucleic acids could be enhanced by incorporating multiple anchoring groups on each probe; however, surface attachment at multiple points will undoubtedly induce configurational constraints that may hinder hybridization to target (Mir and Southern, 1999; Southern et al., 1999).

In summary, the following key points pertain to post-MCH-treated samples. First, even non-thiolated ssDNA is not displaced completely by MCH, suggesting an incomplete MCH monolayer containing 5 to 15% of the initially adsorbed ssDNA. Second, surface coverage of thiolated samples is highly sensitive to probe length above 16 bases, dropping by more than an order of magnitude for probe lengths from 16 to 48 nucleotides. Third, the displacing action of MCH is the dominant factor in determining final probe coverage; electrostatic interprobe repulsions are of less importance (Fig. 5).

CONCLUSIONS

The present study investigated the relationship between probe surface density and length for ssDNA oligonucleotides 8 to 48 nucleotides long. Immobilized coverages, on gold surfaces, of oligonucleotides bearing a 5′ terminal thiol

group were contrasted with those of unmodified ssDNA. Changes in immobilized amounts arising from displacement of adsorptive contacts between ssDNA nucleotides and the gold by a small, thiol-functionalized organic molecule (mercaptohexanol) were also examined.

Comparison of immobilized amounts for ssDNA with and without a 5′ hexanethiol linker on bare gold show that the thiol enhances oligonucleotide adsorption by about an order of magnitude. However, the effectiveness of the single thiol anchoring group at driving immobilization decreases as the length of the oligonucleotide is increased. For sufficiently long adsorption times (20 h in the present study), thiolated oligonucleotides shorter than about 24 bases organize such that their surface density is only weakly dependent on probe length. In this regime, the surface density is about half of the theoretical, close-packed maximum. These high surface densities are consistent with oligonucleotides organizing in an end-attached configuration where each ssDNA strand is bound to the substrate solely through its 5′ thiol. For longer oligonucleotides, this simple picture breaks down as the polymeric nature of the ssDNA strands begins to manifest, leading to a decrease in surface coverage with probe length.

A portion of this work was conducted by Gene Logic's Chip Research and Development Group within the Research and Development Division. A. S. would like to acknowledge a National Research Council postdoctoral fellowship at the National Institute of Standards and Technology (NIST). We would also like to thank Dr. Stanley Abramowitz of the Advanced Technology Program at NIST for his support of the work at NIST.

Certain commercial products and instruments are identified to adequately specify the experimental procedure. In no case does such identification imply endorsement by the authors or NIST.

REFERENCES

Bamdad, C. 1997. The use of variable density self-assembled monolayers to probe the structure of a target molecule. *Biophys. J.* 75:1989–1996.

Bamdad, C. 1997. A DNA self-assembled monolayer for the specific attachment of unmodified double- or single-stranded DNA. *Biophys. J.* 75:1997–2003.

Bard, A. J., and L. R. Faulkner. 1980. Electrochemical Methods. John Wiley and Sons, New York.

Chan, V., D. J. Graves, P. Fortina, and S. E. McKenzie. 1997. Adsorption and surface diffusion of DNA oligonucleotides at liquid/solid interfaces. *Langmuir.* 13:320–329.

Cheung, V., M. Morley, F. Aguilar, A. Massimi, R. Kucherlapati, and G. Childs. 1999. Making and reading microarrays. *Nat. Genet.* (suppl.) 21:15–19.

Cohen Stuart, M. A., and G. J. Fleer. 1996. Adsorbed Polymer Layers in Nonequilibrium Situations. *Annu. Rev. Mater. Sci.* 26:463–500.

Cotton, C., A. Glidle, G. Beamson, and J. M. Cooper. 1998. Dynamics of the formation of mixed alkanethiol monolayers: Applications in structuring biointerfacial arrangements. *Langmuir.* 14:5139–5146.

Duggan, D., M. Bittner, Y. Chen, P. Meltzer, and J. Trent. 1999. Expression profiling using cDNA microarrays. *Nat. Genet.* (suppl.) 21:10–14.

Gingeras, T. R., D. Y. Kwoh, and G. R. Davis. 1987. Hybridization properties of immobilized nucleic acids. *Nucleic Acids Res.* 15: 5373–5390.

Herne, T. M., and M. J. Tarlov. 1997. Characterization of DNA probes immobilized on gold surfaces. *J. Am. Chem. Soc.* 119:8916–8920.

Kelley, S. O., J. K. Barton, N. M. Jackson, and M. G. Hill. 1997. Electrochemistry of methylene blue bound to a DNA-modified electrode. *Bioconjugate Chem.* 8:31–37.

Leff, D. V., L. Brandt, and J. R. Heath. 1996. Synthesis and characterization of hydrophobic, organically-soluble gold nanocrystals functionalized with primary amines. *Langmuir.* 12:4723–4730.

Levicky, R., T. M. Herne, M. J. Tarlov, and S. K. Satija. 1998. Using self-assembly to control the structure of DNA monolayers on gold: A neutron reflectivity study. *J. Am. Chem. Soc.* 120:9787–9792.

Lipshutz, R., S. Fodor, T. Gingeras, and D. Lockhart. 1999. High density synthetic oligonucleotide arrays. *Nat. Genet.* (suppl.) 21:20–24.

Mir, K. U., and E. M. Southern. 1999. Determining the influence of structure on hybridization using oligonucleotide arrays. *Nat. Biotechnol.* 17:788–792.

Mucic, R. C., M. K. Herrlein, C. A. Mirkin, and R. L. Letsinger. 1996. Synthesis and characterization of DNA with ferrocenyl groups attached to their 5′-termini: electrochemical characterization of a redox-active nucleotide monolayer. *Chem. Commun.* 1996:555–557.

O'Donnell, M. J., K. Tang, H. Koster, C. L. Smith, and C. R. Cantor. 1997. High-density, covalent attachment of DNA to silicon wafers for analysis by MALDI-TOF mass spectrometry. *Anal. Chem.* 69:2438–2443.

Pease, A. C., D. Solas, E. J. Sullivan, M. T. Cronin, C. P. Holmes, and S. Fodor. 1994. Light-generated oligonucleotide arrays for rapid DNA sequence analysis. *Proc. Natl. Acad. Sci. USA.* 91:5022–5026.

Peterlinz, K. A., R. M. Georgiadis, T. M. Herne, and M. J. Tarlov. 1997. Observation of hybridization and dehybridization of thiol-tethered DNA using two-color surface plasmon resonance spectroscopy. *J. Am. Chem. Soc.* 119:3401–3402.

Record, M. T., Jr., C. F. Anderson, and T. M. Lohman. 1978. Thermodynamic analysis of ion effects on the binding and conformational equilibria of proteins and nucleic acids: the roles of ion association or release, screening, and ion effects on water activity. *Quarterly Rev. Biophys.* 11:103–178.

Rekesh, D., Y. Lyubchenko, L. Shlyakhtenko, and S. M. Lindsay. 1996. Scanning tunneling microscopy of mercapto-hexyl-oligonucleotides attached to gold. *Biophys. J.* 71:1079–1086.

Southern, E. M., S. C. Case-Green, J. K. Elder, M. Johnson, K. U. Mir, L. Wang, and J. C. Williams. 1994. Arrays of complementary oligonucleotides for analysing the hybridisation behaviour of nucleic acids. *Nucleic Acids Res.* 22:1368–1373.

Southern, E. M., K. U. Mir, and M. Shchepinov. 1999. Molecular interaction on microarrays. *Nat. Genet.* (suppl.) 21:5–9.

Steel, A. B., T. M. Herne, and M. J. Tarlov. 1998. Electrochemical quantitation of DNA immobilized on gold. *Anal. Chem.* 70:4670–4677.

Tarlov, M. J., D. R. Burgess, and G. Gillen. 1993. UV Photopatterning of alkanethiolate monolayers self-assembled on gold and silver. *J. Am. Chem. Soc.* 115:5305–5306.

Tinland, B., A. Pluen, J. Sturm, and G. Weill. 1997. Persistence length of single-stranded DNA. *Macromolecules.* 30:5763–5765.

Ulman, A. 1996. Formation and Structure of Self-Assembled Monolayers. *Chem. Rev.* 96:1533–1554.

Xu, C., L. Sun, L. J. Kepley, and R. M. Crooks. 1993. Molecular Interactions between Organized, Surface-Confined Monolayers and Vapor-Phase Probe Molecules. 6. In-situ FTIR External Reflectance Spectroscopy of Monolayer Adsorption and Reaction Chemistry *Anal. Chem.* 65:2102–2107.

Williams, J. C., S. C. Case-Green, K. U. Mir, and E. M. Southern. 1994. Studies of oligonucleotide interactions by hybridisation to arrays: The influence of dangling ends on duplex yield. *Nucleic Acids Res.* 22: 1365–1367.